Microchimica Acta (2019) 186: 837
https://doi.org/10.1007/s00604-019-3983-7

ORIGINAL PAPER

A system composed of vanadium(IV) disulfide quantum dots and molybdenum(IV) disulfide nanosheets for use in an aptamer-based fluorometric tetracycline assay

Xiaohan Ma[1] · Cuicui Du[1] · Jinling Zhang[1] · Mengxiang Shang[1] · Wenbo Song[1]

Received: 14 June 2019 / Accepted: 28 October 2019 / Published online: 23 November 2019

Abstract

A system composed of vanadium(IV) disulfide quantum dots (VS_2 QDs) and molybdenum(IV) disulfide (MoS_2) nanosheets for use in an aptamer-based fluorometric tetracycline assay was developed. The tetracycline (TET) aptamer was first immobilzed on the VS_2 QDs with a typical size of 3 nm. The blue fluorescence of the VS_2 QDs (labeled with aptamer) with emission maxima at 448 nm (under excitation at 360 nm) was subsequently quenched by MoS_2 nanosheets. If TET is recognized by the aptamer, the VS_2 QDs drift away from the basal plane of the MoS_2 nanosheets. This generated "turn-on" fluorescence of the VS_2 QDs. A VS_2 QD/MoS_2 nanosheet-based fluorometric TET aptasensor was thus constructed. Selective and sensitive TET bioanalysis was realized in a linear range of 1 to 250 ng mL^{-1}. The detection limit was 0.06 ng mL^{-1}. Its applicability of determination of TET in milk samples has been demonstrated.

Keywords VS_2 quantum dots · MoS_2 · Aptamer · Turn-on fluorescence · Fluorometric assay · Antibiotic

Introduction

Tetracycline (TET) is produced by actinomycetes. It can inhibit the peptide chain extension and bacterial protein synthesis. Because of the effective antimicrobial properties, few side effect and low price, it has been widely used in the treatment of infectious diseases in humans and animals [1]. Nowadays, the abuse of TET has caused serious environmental and health problems [2]. For instance, the antibiotic residues in daily foods such as meat, milk, honey, fish and eggs [3] may lead to the accumulation of TET in human. This will cause damage to the digestive tract and liver, affect the development of the skeleton, and weaken the immune system function [4]. In this concern, China has set the maximum residue limit of TET residues in honey and milk or muscle tissue to 50 μg kg^{-1}, 100 μg kg^{-1}, respectively [5]. Exploring effective sensing approach to facile monitor TET is hence imperative.

Various techniques, including high performance liquid chromatography (HPLC), gas chromatography-mass spectrometry (GC-MS), capillary electrophoresis (CE) and enzyme-linked immunosorbent assay (ELISA) etc. have been developed for TET detection [6–10]. By comparison, the recently emerged aptamer-based bioanalytical method attracts extensive attention [11]. The aptamers are 3D structured single-stranded oligonucleotides. They are normally synthesized by Systematic Evolution of Ligands by Exponential enrichment (SELEX) with high affinity and specificity [12]. Compared with protein antibodies and enzymes, the aptamers can be cost-effectively synthesized with high purity and reproducibility. Besides, they also have advantages of small size, high stability, easy to modify, long-term preservation and without immunogenicity [13]. These attributes enable them to be promising in aptamer-based bioanalysis with high affinity and reproducibility [14]. Luo et al. developed CS-AuNPs probe for colorimetric aptasensing of tetracycline [15]. Xu et al. reported a ferrocene/carbon nanofbers-based ratiometric electrochemical aptasensor for detection of tetracycline residues [16]. Despite of the progress, developing new bioassay system for sensitive and specific determination of antibiotics is still a challenge.

Electronic supplementary material The online version of this article (https://doi.org/10.1007/s00604-019-3983-7) contains supplementary material, which is available to authorized users.

✉ Wenbo Song
wbsong@jlu.edu.cn

[1] College of Chemistry, Jilin University, Changchun 130012, People's Republic of China

Ultrathin two-dimensional (2D) transition metal chalcogenides and transition metal oxides have gained increased attention in the fields of electronics, sensors and catalysis [17]. Particular research interest has focused on integrating these 2D nanosheets into biosensors, stemming from unique structural and electrical properties combing with high loading efficiency for biomolecules [18]. Generally, most transition metal nanosheets have the ability to quench fluorescence, through energy-transfer or electron-transfer from excited fluorophores to nanosheets. And more importantly, the large surface area of 2D nanomaterial can offer more quenching sites, enabling high quenching efficiency and detection sensitivity [19]. Both theoretical calculations and experimental studies have demonstrated that MoS_2 nanosheets can physically adsorb aromatic compounds (such as pyridine or purine) and conjugated compounds [20]. Zhu and co-workers have reported high affinity of single-stranded DNA (ssDNA) to MoS_2 nanosheets, through Van der Waals interactions between lamellar planes and bases. They also demonstrated that MoS_2 nanosheets have a high fluorescence quenching capability towards dye labeled-ssDNA [21]. Herein, a system of VS_2 QD/MoS_2 nanosheets for use in an aptamer-based fluorometric tetracycline assay has been developed. The TET aptamers were first fabricated on the surfaces of VS_2 QDs. Then, the fluorescence of TET aptamer labeled VS_2 QDs was quenched by MoS_2 nanosheets. When the TET was specifically recognized by the aptamer, the VS_2 QDs may be taken away from the MoS_2 nanosheets. This will lead to "turn-on" fluorescence of the VS_2 QDs. A VS_2 QD/MoS_2 nanosheets-based fluorescent aptasensing platform for TET is thus constructed.

Experimental section

Chemicals and instrumentation

Specific details of chemicals and instrumentation are provided in the electronic supplementary material. The MoS_2 nanosheets were thermolytically obtained following our previously reported method [22]. The VS_2 QDs were synthesized via a one-step hydrothermal approach [23]. The concentration of VS_2 QDs is ~2.2 mg mL^{-1} after purification by silica gel column chromatography. Related details can also be found in the electronic supplementary material.

Fabrication of aptamer-labeled VS_2 QDs

The condensation reaction between amino and carboxyl groups [24] is involved to fabricate the TET aptamer labeled VS_2 QDs. The detailed procedures can be described as follows: First, 100.0 μL of 500 mM EDC was added into 1.0 mL of VS_2 QD suspension (~2.2 mg mL^{-1}), and the final concentration of QD suspension was 2.0 mg mL^{-1}. Second, the mixture was continuously stirred for 30 min to activate the carboxyl group on the QD surface. Third, 0.9 mL of Tris-HCl was added, the resulting concentration of the carboxyl-activated VS_2 QD suspension was 1.0 mg mL^{-1} (2.0 mL, ~3.7 μM). Finally, incubation of the TET aptamer (3.0 μM) with carboxyl-activated VS_2 QDs at room temperature for 15 min, the TET aptamer labeled VS_2 QDs were achieved.

Aptamer-based fluorometric tetracycline assay

In a typical process, 2.0 mL of TET aptamer labeled VS_2 QDs (1.0 mg mL^{-1}, ~3.7 μM) was first mixed with 30.0 μL of 0.2 mg mL^{-1} MoS_2 nanosheets. Then, 50.0 μL TET solution with tunable concentration was added and mixed thoroughly. After each sample reacted for 25 min under room temperature, the fluorescence emission was measured under the excitation of 360 nm.

Selectivity

The selectivity of the aptamer-based fluorometric TET assay towards several antibiotics (such as OTC, DOX, KAN, OFX, PNC and CIP) was investigated. Briefly, the fluorescence of the VS_2 QDs quenched by MoS_2 nanosheets (3.0 μg mL^{-1}) was recorded as the initial intensity. After addition of 50 μL (20 μg mL^{-1}) each of the interferential species into the solution (2.0 mL), the fluorescence intensity was recorded again.

TET assay in milk samples

Milk samples were supplied from retail supermarket (Changchun, China) and treated by the following steps. Briefly, 5.0 mL raw milk was mixed with EDTA's McLinin Protein Buffer (50 μL 400 mM, pH = 5). To deposit protein and dissolve fat and other organic substances in the sample matrix, 20.0 mL trichloroacetic acid was added and mixed for 1 min. The mixture was then centrifuged at 8000 rpm for 20 min to remove the protein, fat and other organic substances. The pH of supernatant was adjusted to 7.5 by 1 M NaOH solution. After filtration, the final solution was used for detection. A certain amount of TET was spiked into the raw milk. The spiked sample was pretreated and analyzed similarly.

Results and discussion

Fluorescence of aptamer-labeled VS_2 QDs

The synthesis and characterization of water-soluble monolayer MoS_2 QDs have been reported in our previous work [25]. Pronounced blue-shift of excitonic absorption

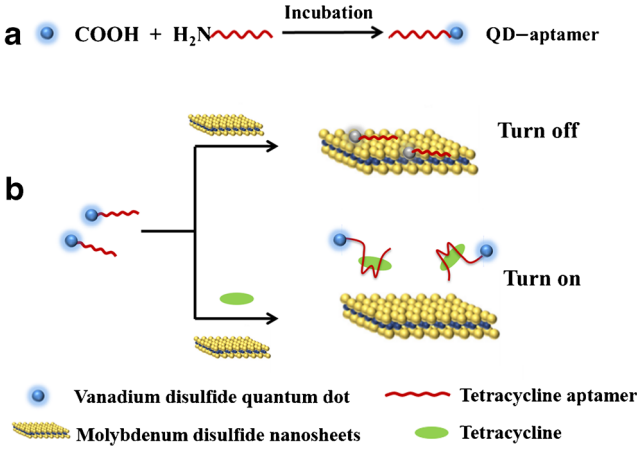

Scheme 1 Schematic representation of the preparation of aptamer labeled VS_2 QD (a) for aptamer-based fluorometric tetracycline assay (b).

beyond single-layer MoS_2 nanosheets and unusual up-conversion photoluminescence at room temperature were unprecedentedly discovered. Following the modified procedures, we prepared VS_2 QDs with a relative uniform size of ~3 nm (Fig. S1a and S1b) similarly. Detailed structural characterization, luminescence behavior and promising applications for glutathione and tetracycline determination can be found in recent reports [23, 26]. In this work, another system composed of VS_2 QDs and MoS_2 nanosheets has been designed for use in aptamer-based fluorometric assay. Specific determination of tetracycline in practical samples has been exemplified.

For analyte determination, the aptamer labeled VS_2 QDs was first prepared via the condensation reaction of carboxyl-activated VS_2 QDs and amino-terminated TET aptamer. Scheme 1a shows the schematic illustration of the fabrication of the aptamer labeled VS_2 QDs. In Fig. 1a, the aptamer labeled VS_2 QDs exhibits a similar emission peak at around 448 nm (blue light) with the VS_2 QDs under an excitation wavelength of 360 nm. While the fluorescence intensity slightly declines compared to the primary one. When the aptamer labeled VS_2 QDs was stored in the dark at 4 °C for 5, 10, 15, 20 days, imperceptible changes in the fluorescence intensity are observed (Fig. 1b). This result indicates that the aptamer labeled VS_2 QDs have a good stability in aqueous solution.

The MoS_2 nanosheets were synthesized via pyrolysis of ammonium molybdate, a layered C_3N_4 template and sulfur source under a N_2 atmosphere [22]. The characteristic ultrathin structure of these nanosheets can be clearly seen from Fig. S2a. Well-resolved crystal lattice with an interplanar spacing of 0.62 nm can be assigned to the distance of (002) crystal plane of hexagonal MoS_2. All the diffraction peaks in Fig. S2b can be indexed to the crystalline planes of hexagonal MoS_2 (ICDD, reference number, 00–006–0097). The UV-visible absorption spectrum of MoS_2 nanosheets reveals a wide absorption in the range of 350 nm to 600 nm. This absorption spectrum is extensively overlapped with the emission spectrum of the aptamer labeled VS_2 QDs (Fig. 2a). This behavior implies a possibility of VS_2 QD fluorescence quenching by MoS_2 nanosheets. Figure 2b compares the fluorescence intensity change of the aptamer labeled VS_2 QDs in the absence or presence of MoS_2 nanosheets. Extensively weakened fluorescence is observed in the presence of MoS_2 nanosheets, since the emitted fluorescence of the VS_2 QDs is partially absorbed by the MoS_2 nanosheets and the fluorescence is thus quenched.

To explore the possible mechanism of fluorescence quenching, the lifetime of the aptamer labeled QD emission was measured and compared with that of the aptamer labeled VS_2 QD/MoS_2 nanosheets. The fluorescence lifetime of the composite system decreases (Fig. 3), indicating that the fluorescence decay cannot be ascribed to static quenching and inner filter effect [27]. Although the estimated distance between acceptor and donor is less than 10 nm (detailed calculation can be found in the Electronic Supporting Material), the possibility of fluorescence quenching by photoinduced electron transfer still cannot be excluded. More efforts are required in near future to explore the exact mechanism.

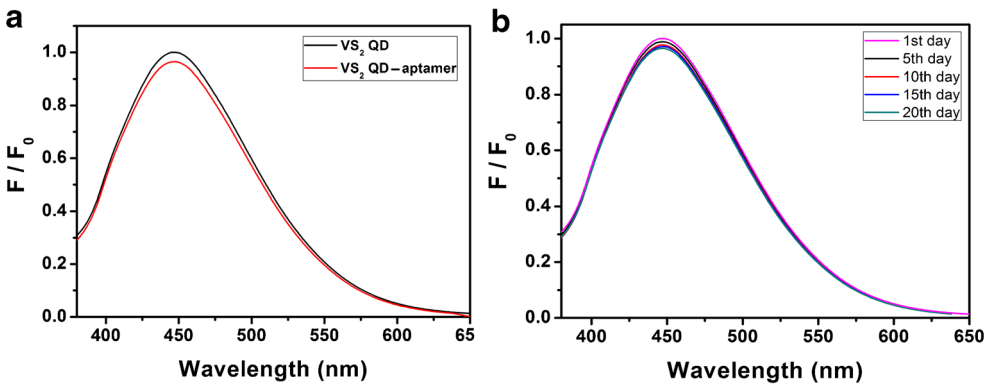

Fig. 1 **a** Fluorescence emission spectra of VS_2 QDs and aptamer labeled VS_2 QDs under the same condition. **b** The photostability of aptamer labeled VS_2 QDs during 20 days.

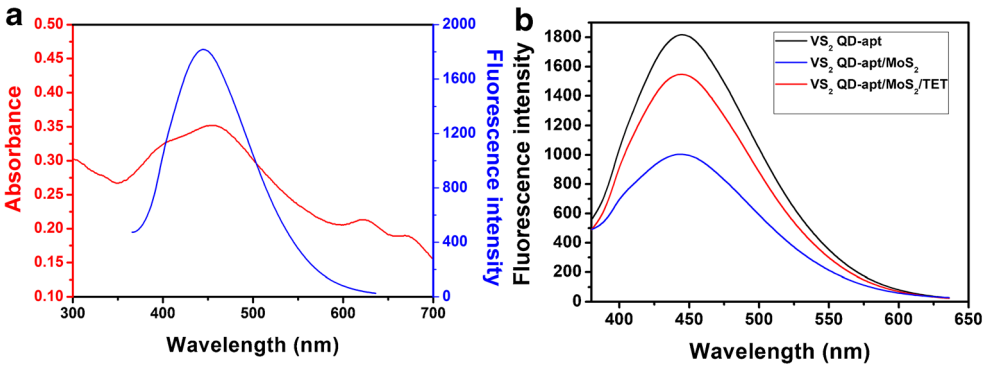

Fig. 2 **a** UV − vis absorption spectrum of MoS_2 nanosheets and fluorescence emission spectrum of aptamer labeled VS_2 QDs. **b** The fluorescence spectra of aptamer labeled VS_2 QDs and aptamer labeled VS_2 QD/MoS_2 nanosheet without and with TET.

Aptamer-based fluorometric TET assay

The change in fluorescence intensity of the aptamer labeled VS_2 QD/MoS_2 system in the presence of TET is studied. Figure 2b depicts that remarkable fluorescence recovery is realized in the presence of 600 ng mL^{-1} TET. The specific recognition between TET and the aptamer leads to the VS_2 QDs detached from the surface of MoS_2 nanosheets. The fluorescence is therefore recovered. By monitoring the turn-on fluorescence intensity, the TET may thus be detected.

The mechanism of the aptamer labeled VS_2 QD/MoS_2 nanosheets for TET detection is schematically represented in Scheme 1b. In the scheme, the interactions between all the species are also indicated. The VS_2 QD probe emits intense blue light at 448 nm under UV light excitation of 360 nm. The MoS_2 nanosheet serves as fluorescence quenching species. The TET aptamer labeled VS_2 QDs are adsorbed on the surfaces of MoS_2 nanosheets through van der walls force, the fluorescence under 360 nm excitation is efficiently quenched. When the molecular recognition between TET and the aptamer labeled VS_2 QDs takes place, well-folded TET-aptamer complex is formed. The conformation change of the complex decreases the exposure of nucleobases, the VS_2 QDs are detached from the surface of MoS_2 nanosheets. The fluorescence of the VS_2 QD probe is thus restored.

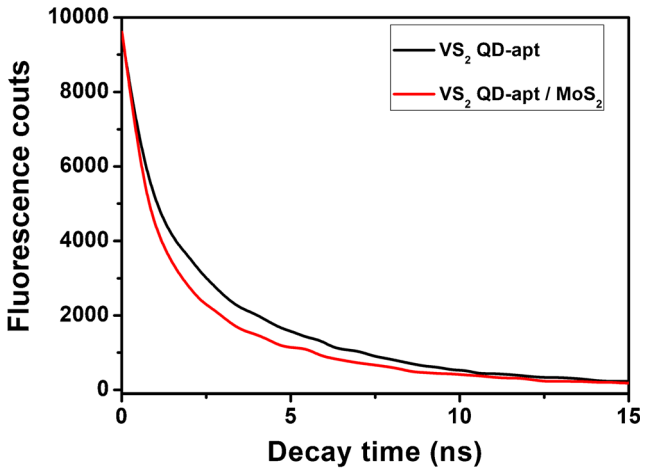

Fig. 3 The lifetime change of the aptamer labeled VS_2 QDs and aptamer labeled VS_2 QD/MoS_2 nanosheet.

Optimization of assay conditions

The following parameters are optimized: (a) concentration of MoS_2; (b) incubation time; (c) tetracycline aptamer concentration; (d) sample pH value. Respective text and Figures on optimization are shown in Fig. S3 in the Electronic Supporting Material. In short, the following experimental conditions are found to give best results: (a) optimal concentration of MoS_2: 3 μg mL^{-1}; (b) optimal incubation time: 25 min; (c) optimal tetracycline aptamer concentration: 3 μM; (d) best sample pH value: 7.5.

TET aptasensing performances

Under optimal conditions, fluorescence detection of TET was carried out. Figure 4a shows the tunable fluorescence spectra towards different concentration of TET. The small inset magnified the fluorescence emission behavior at low TET concentration. The plot of TET concentration-dependent fluorescence intensity is presented in Fig. 4b. A good linear relationship between the fluorescence intensity and TET concentration in the range from 1 to 250 ng mL^{-1} can be observed in Fig. 4c. The linear regression equation is $FL = 1.67 \times C_{TET}$ (ng mL^{-1}) + 1007.22. The correlation coefficient is 0.9982. A detection limit of 0.06 ng mL^{-1} is achieved (3δ/S, δ is the standard deviation of the blank signal and S is the slope of the linear calibration plot). Compared with most of the aptasensing approaches for the detection of TET, the VS_2 QD/MoS_2 aptamer-based fluorescent assay exhibits a relatively low detection limit (Table 1), showing a promise in food quality and safety control.

Selectivity study

A series of derivatives with similar structure to tetracycline (such as OTC, DOX, KAN, OFX, PNC and CIP) are selected to evaluate the possible interference effect on the determination of TET. Under above conditions, 50 μL of 20 g mL^{-1} TET and each of

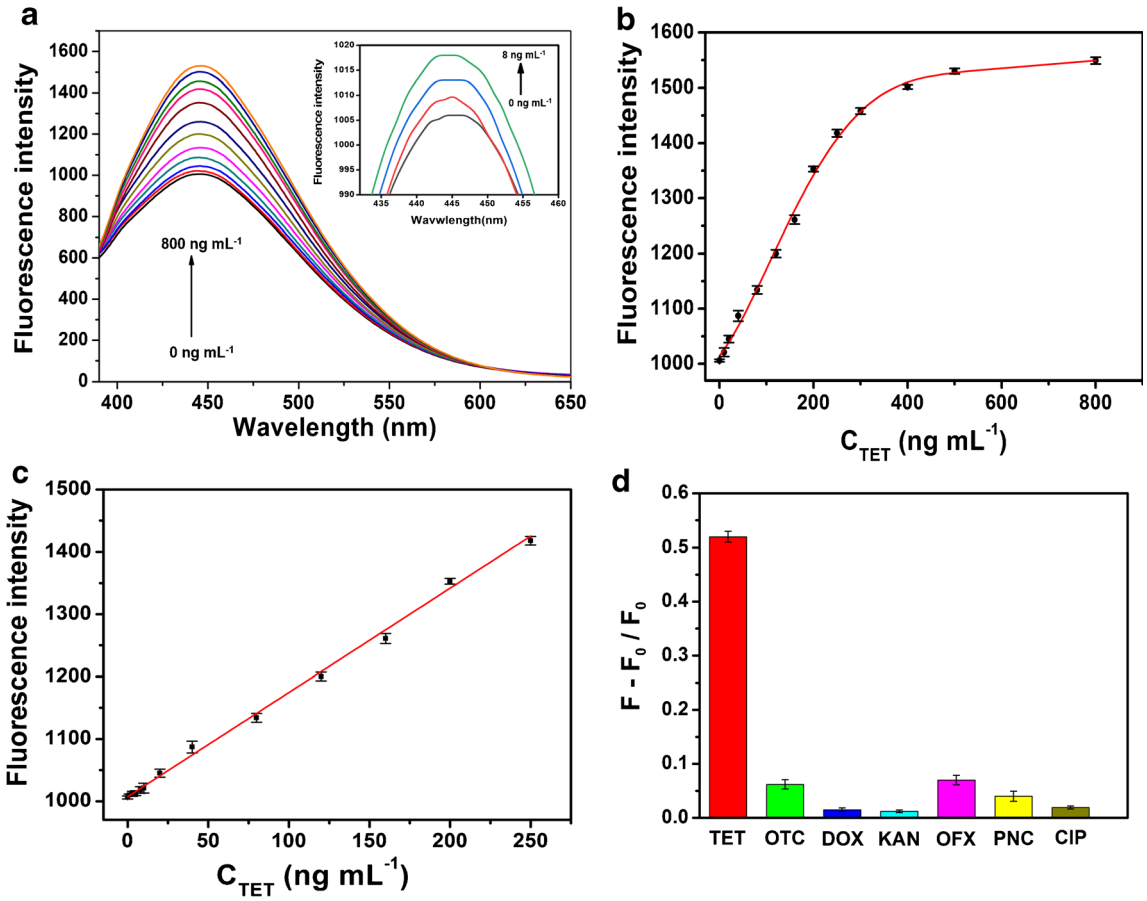

Fig. 4 **a** The change of fluorescence spectra with TET concentration. **b** The trend of fluorescence recovery with TET concentration. **c** The linear relationship between emission intensity and TET concentration. **d** The specificity of VS_2 QD-based aptasensor towards a series of structurally similar tetracycline derivatives.

the antibiotics were added, and the fluorescence intensity was recorded. All data are obtained based on three repetitive measurements. As shown in Fig. 4d, none of these antibiotics causes obvious fluorescence increase. Above study demonstrates a high specificity to tetracycline over other antibiotics, since the aptamer can distinguish even minor structural difference between the target and its analog [31].

Detection of TET in milk samples

To further demonstrate the possibility of the aptasensor for practical application, the concentrations of TET in several milk samples were detected. Since the tetracycline veterinary drugs in all the milk samples are found below the detection limit, a series of spiked samples were prepared by addition of 50 μL different concentration of TET. For each concentration of TET (5 ng mL^{-1}, 20 ng mL^{-1}, 50 ng mL^{-1} and 100 ng mL^{-1}), three replicate samples were prepared. Under the optimal conditions, the TET concentration of each spiked sample was detected. The relative standard deviation and spiked recovery are presented in Table 2. The recovery of TET is in the range of 96.7–107.1%. The relative standard deviation (RSD) is less than 3.22%.

Table 1 TET assay performances compared with other fluorescent sensing approaches

Method	Linear range	LOD	Ref.
Polyethyleneimine capped bimetallic Au/Pt nanoclusters	0.5–10 ng mL^{-1}	0.35 ng mL^{-1}	[28]
FICA with ZnCdSe/ZnS QD	20–100 ng mL^{-1}	20 ng mL^{-1}	[29]
Fluorescent TET detection using dually emitting carbon dots	0.48–14.4 μg mL^{-1}	0.25 ng mL^{-1}	[30]
VS_2 QD/MoS_2 aptamer-based fluorescent assay	1–250 ng mL^{-1}	0.06 ng mL^{-1}	This work

Table 2 The results of TET detection in milk samples

Samples	Added (ng mL^{-1})	Measured (ng mL^{-1})	Recovery (%)	RSD (%)
1	5.00	5.26	105.2	2.23
2	20.00	21.42	107.1	3.22
3	50.00	48.37	97.7	1.89
4	100.00	95.68	96.7	1.60

Conclusions

Using MoS_2 nanosheets as an efficient quencher to the blue fluorescence of VS_2 QDs, a VS_2 QD/MoS_2 nanosheets-based aptasensor for TET determination was developed. The specific recognition between aptamer and target resulted in an increase of the distance between the VS_2 QDs and MoS_2 nanosheets. The VS_2 QDs were thus detached from the MoS_2 nanosheets, and the fluorescence was recovered. This aptamer-based fluorescent assay approach has advantages of high sensitivity, low detection limit and high specificity. Its feasibility of determination of TET in milk samples has been demonstrated. Note that, the interference caused by biomatter is a disadvantage for the method working in the UV (excitation at 360 nm). Many samples display strong background UV absorption and fluorescence. In this regards, the UV light used for fluorescence excitation could be screened off by UV absorbers, which may weaken the signal. Thus, there still exists a limitation of the present approach in practical application.

Acknowledgments This work was supported by the National Natural Science Foundation of China (No. 21874053 and No. 21475051).

Compliance with ethical standards

Conflict of interest The authors declare that they have no conflict of interest.

References

1. Liu Y, Yan K, Zhang JD (2016) Graphitic carbon nitride sensitized with CdS quantum dots for visible-light-driven Photoelectrochemical Aptasensing of tetracycline. ACS Applied Materials & Interfaces 8(42):28255–28264
2. Benvidi A, Tezerjani MD, Moshtaghiun SM, Mazloum-Ardakani M (2016) An aptasensor for tetracycline using a glassy carbon modified with nanosheets of graphene oxide. Microchimica Acta 183:1797–1804
3. Peres GT, Rath S, Reyes FGR (2010) A HPLC with fluorescence detection method for the determination of tetracyclines residues and evaluation of their stability in honey. Food Control 21(5):620–625
4. Shen L, Chen J, Li N, He PL, Li Z (2014) Rapid colorimetric sensing of tetracycline antibiotics with in situ growth of gold nanoparticles. Analytica Chimica Acta 839:83–90
5. Guo ZY, Gai PP (2011) Development of an ultrasensitive electrochemiluminescence inhibition method for the determination of tetracyclines. Analytica Chimica Acta 688(2):197–202
6. Cinquina AL, Longo F, Anastasi G, Giannetti L, Cozzani R (2003) Validation of a high-performance liquid chromatography method for the determination of oxytetracycline, tetracycline, chlortetracycline and doxycycline in bovine milk and muscle. Journal of Chromatography. A 987(1–2):227–233
7. Ternes TA (2001) Analytical methods for the determination of pharmaceuticals in aqueous environmental samples. Trac-Trend Anal Chem 20(8):419–434
8. Kowalski P (2008) Capillary electrophoretic method for the simultaneous determination of tetracycline residues in fish samples. J Pharmaceut Biomed 47(3):487–493
9. Aga DS, Goldfish R, Kulshrestha P (2003) Application of ELISA in determining the fate of tetracyclines in land-applied livestock wastes. Analyst 128(6):658–662
10. Tan HL, Ma CJ, Song YH, Xu FG, Chen SH, Wang L (2013) Determination of tetracycline in milk by using nucleotide/lanthanide coordination polymer-based ternary complex. Biosensors & Bioelectronics 50:447–452
11. He F, Tang YL, Wang S, Li YL, Zhu DB (2005) Fluorescent amplifying recognition for DNA G-quadruplex folding with a cationic conjugated polymer: a platform for homogeneous potassium detection. Journal of the American Chemical Society 127(35):12343–12346
12. Alves RD, Romero-González R, López-Ruiz R, Jiménez-Medina ML, Frenich AG (2016) Fast determination of four polar contaminants in soy nutraceutical products by liquid chromatography coupled to tandem mass spectrometry. Analytical and Bioanalytical Chemistry 408(28):8089–8098
13. Bai YF, Feng F, Zhao L, Wang CY, Wang HY, Tian MZ, Qin J, Duan YL, He XX (2013) Aptamer/thrombin/aptamer-AuNPs sandwich enhanced surface plasmon resonance sensor for the detection of subnanomolar thrombin. Biosensors & Bioelectronics 47:265–270
14. Zhao HM, Gao S, Liu M, Chang YY, Fan XF, Quan X (2013) Fluorescent assay for oxytetracycline based on a long-chain aptamer assembled onto reduced graphene oxide. Microchimica Acta 180(9–10):829–835
15. Luo Y, Xu JY, Li Y (2015) A novel colorimetric aptasensor using cysteamine stabilized gold nanoparticles as probe for rapid and specific detection of tetracycline in raw milk. Food Control 54:7–15
16. Xu QC, Liu ZN, Fu JY, Zhao WP, Guo YM, Sun X, Zhang HY (2017) Ratiometric electrochemical aptasensor based on ferrocene and carbon nanofibers for highly specific detection of tetracycline residues. Sci rep-Uk 7. Doi:Artn 14729
17. Li H, Yin ZY, He QY, Li H, Huang X, Lu G, Fam DWH, Tok AIY, Zhang Q, Zhang H (2012) Fabrication of single- and multilayer MoS2 film-based field-effect transistors for sensing NO at room temperature. Small 8(1):63–67
18. Ataca C, Ciraci S (2011) Functionalization of single-layer MoS2 honeycomb structures. Journal of Physical Chemistry C 115(27):13303–13311
19. Rurack K (2001) Flipping the light switch 'ON' - the design of sensor molecules that show cation-induced fluorescence enhancement with heavy and transition metal ions. Spectrochimica Acta A 57(11):2161–2195
20. Lorente JA, Valenzuela H, Morote J, Gelabert A (1999) Serum bone alkaline phosphatase levels enhance the clinical utility of prostate

specific antigen in the staging of newly diagnosed prostate cancer patients. European Journal of Nuclear Medicine 26(6):625–632
21. Zhu CF, Zeng ZY, Li H, Li F, Fan CH, Zhang H (2013) Single-layer MoS2-based Nanoprobes for homogeneous detection of biomolecules. Journal of the American Chemical Society 135(16):5998–6001
22. Huang H, Feng X, Du CC, Song WB (2015) High-quality phosphorus-doped MoS2 ultrathin nanosheets with amenable ORR catalytic activity. Chemical Communications 51(37):7903–7906
23. Ma XH, Du CC, Shang MX, Song WB (2018) VS2 quantum dot label-free fluorescent probe for sensitive and selective detection of ALP. Analytical and Bioanalytical Chemistry 410(5):1417–1426
24. Chen TX, Ning F, Liu HS, Wu KF, Li W, Ma CB (2017) Label-free fluorescent strategy for sensitive detection of tetracycline based on triple-helix molecular switch and G-quadruplex. Chinese Chemical Letters 28(7):1380–1384
25. Huang H, Du CC, Shi HY, Feng X, Li J, Tan YL, Song WB (2015) Water-soluble monolayer molybdenum disulfide quantum dots with Upconversion fluorescence. Particle and Particle Systems Characterization 32(1):72–79
26. Du CC, Shang AQ, Shang MX, Ma XH, Song W (2018) Water-soluble VS2 quantum dots with unusual fluorescence for biosensing. Sensors and Actuators B: Chemical 255:926–934
27. Zu FL, Yan FY, Bai ZG, Xu JX, Wang YY, Huang YC, Zhou XG (2017) The quenching of the fluorescence of carbon dots: a review on mechanisms and applications. Microchimica Acta 184:1899–1914
28. Xu N, Meng L, Li HW, Lu DY, Wu YQ (2018) Polyethyleneimine capped bimetallic au/Pt nanoclusters are a viable fluorescent probe for specific recognition of chlortetracycline among other tetracycline antibiotics. Microchimica Acta 185:294–302
29. Sheng W, Chang Q, Shi YJ, Duan WX, Zhang Y, Wang S (2018) Visual and fluorometric lateral flow immunoassay combined with a dual-functional test mode for rapid determination of tetracycline antibiotics. Microchimica Acta 185:404–414
30. Qu F, Sun Z, Liu DY, Zhao XE, You JM (2016) Direct and indirect fluorescent detection of tetracyclines using dually emitting carbon dots. Microchimica Acta 183(9):2547–2553
31. Feng CJ, Dai S, Wang L (2014) Optical aptasensors for quantitative detection of small biomolecules: a review. Biosensors & Bioelectronics 59:64–74